



LAWRENCE
LIVERMORE
NATIONAL
LABORATORY

On the Synthesis and Structure of Resorcinol-Formaldehyde Polymeric Networks - Precursors to 3D Carbon Macroassemblies

J. P. Lewicki, C. A. Fox, M. A. Worsley

January 30, 2015

Polymer

Disclaimer

This document was prepared as an account of work sponsored by an agency of the United States government. Neither the United States government nor Lawrence Livermore National Security, LLC, nor any of their employees makes any warranty, expressed or implied, or assumes any legal liability or responsibility for the accuracy, completeness, or usefulness of any information, apparatus, product, or process disclosed, or represents that its use would not infringe privately owned rights. Reference herein to any specific commercial product, process, or service by trade name, trademark, manufacturer, or otherwise does not necessarily constitute or imply its endorsement, recommendation, or favoring by the United States government or Lawrence Livermore National Security, LLC. The views and opinions of authors expressed herein do not necessarily state or reflect those of the United States government or Lawrence Livermore National Security, LLC, and shall not be used for advertising or product endorsement purposes.

On the Synthesis and Structure of Resorcinol- Formaldehyde Polymeric Networks – Precursors to 3D- Carbon Macroassemblies

James P. Lewicki, Christina A. Fox and Marcus A. Worsley

Lawrence Livermore National Laboratory, 7000 East Avenue, Livermore, CA 94510, USA

AUTHOR E-MAIL ADDRESS: James P Lewicki; Lewicki1@llnl.gov

*CORRESPONDING AUTHOR FOOTNOTE. Ph: (925) 960 5100 Fax: email: lewicki1@llnl.gov

ABSTRACT

With the new impetus towards the development of hierarchical graphene and CNT macro-assemblies for application in fields such as advanced energy storage, catalysis and electronics; there is much renewed interest in organic carbon-based sol-gel processes as a synthetically convenient and versatile means of forming three dimensional, covalently bonded organic/inorganic networks. Such matrices can act as highly effective precursors, scaffolds or molecular ‘glues’ for the assembly of a wide variety of functional carbon macro-assemblies. However, despite the utility and broad use of organic sol-gel processes - such as the ubiquitous resorcinol-formaldehyde (RF) reaction, there are details of the reaction chemistries of these important sol-gel processes that remain poorly understood at present. It is therefore both timely and necessary to examine these reactions in more detail using modern analytical

techniques in order to gain a more rigorous understanding of the mechanisms by which these organic networks form. The goal of such studies is to obtain improved and rational control over the organic network structure, in order to better direct and tailor the architecture of the final inorganic carbon matrix. In this study we have investigated in detail, the mechanism of the organic sol-gel network forming reaction of resorcinol and formaldehyde from a structural and kinetic standpoint, by using a combination of real-time high field solution state nuclear magnetic resonance (NMR), low field NMR relaxometry and differential scanning calorimetry (DSC). These investigations have allowed us to track the network formation processes in real-time, gain both detailed structural information on the mechanisms of the RF sol-gel process and a quantitative assessment of the kinetics of the global network formation process. It has been shown that the mechanism, by which the RF organic network forms, proceeds via an initial exothermic step correlated to the formation of a free aromatic aldehyde. The network growth reaction then proceeds in a statistical manner following a first order Arrhenius type kinetic relationship - characteristic of a typical thermoset network poly-condensation process. And despite the relative complexity and ill-defined nature of the formaldehyde starting material, the final network structure is to a large extent, governed by the substitution pattern of the resorcinol molecule.

KEYWORDS: Organic Sol-Gels; NMR; Resorcinol-Formaldehyde

1. INTRODUCTION

Sol-gel chemistries are widely employed as a convenient and versatile means of forming three-dimensional (3-D), covalently bonded organic networks.¹ Such organic sol-gels are the precursor to a family of low density, carbon aerogels² and xerogels^{3,4} with exceptional mechanical, thermal and electrical properties. These inorganic carbon ‘foams’ have, over the last 30 years, received much attention for their potential to serve as inorganic electrolytes⁵, thermally resistant barrier layers⁶, electrodes for energy storage⁷, catalysts⁸, separation media⁹ and even fusion fuel carriers¹⁰. The renewed interest in the last 5 years in applications of the sol-gel process for the formation of inorganic carbon

architectures is largely the result of the push toward the formation of hierarchical 3-D macro-assemblies of novel allotropes of carbon¹¹⁻¹³. Recently it has been demonstrated that both carbon-nanotubes and graphene can be successfully formed into high surface area 3-D macro-assemblies through the application of relatively simple organic sol gel reactions to form, amongst other things, ultra-low density aerogels with unique mechanical, thermal, and electrical properties^{12,13}.

Organic sol-gel processes are typically based on the poly-condensation of multifunctional small molecule precursors in the presence of a suitable solvent, to form a 3-D organic polymeric network. The solvent can be subsequently removed or exchanged resulting in the formation of a xerogel or aerogel structure, respectively - which may be further processed or modified thermally or chemically. The addition of functional, secondary additives such as graphene oxide or single-walled carbon nanotubes during the network forming reaction allow the covalent incorporation of additional carbon architecture into the organic network and is the basis of the synthetic route for the formation of a family of functional 3-D carbon macro-assemblies¹³. By far the most widely employed organic sol-gel process in the field of inorganic, low-density carbon architectures remains the solvent-mediated resorcinol-formaldehyde (RF) polycondensation reaction¹⁴. It is significant that, despite its utility and broad use¹⁴, there are details of the reaction chemistry of the RF sol-gel process that remain poorly understood. While over the last 40 years there has been a concerted effort to define mechanisms and kinetic dependences of inorganic sol-gel processes¹⁵⁻¹⁸, there has been much less progress in understanding organic, sol-gel reactions. There are a number of publications on the early stage reaction mechanisms of the RF reaction¹⁹⁻²², however the mechanisms proposed are general (see **Figure 1**), make large assumptions about the purity and state of the starting material and provide virtually no information on the kinetics of the network formation process.

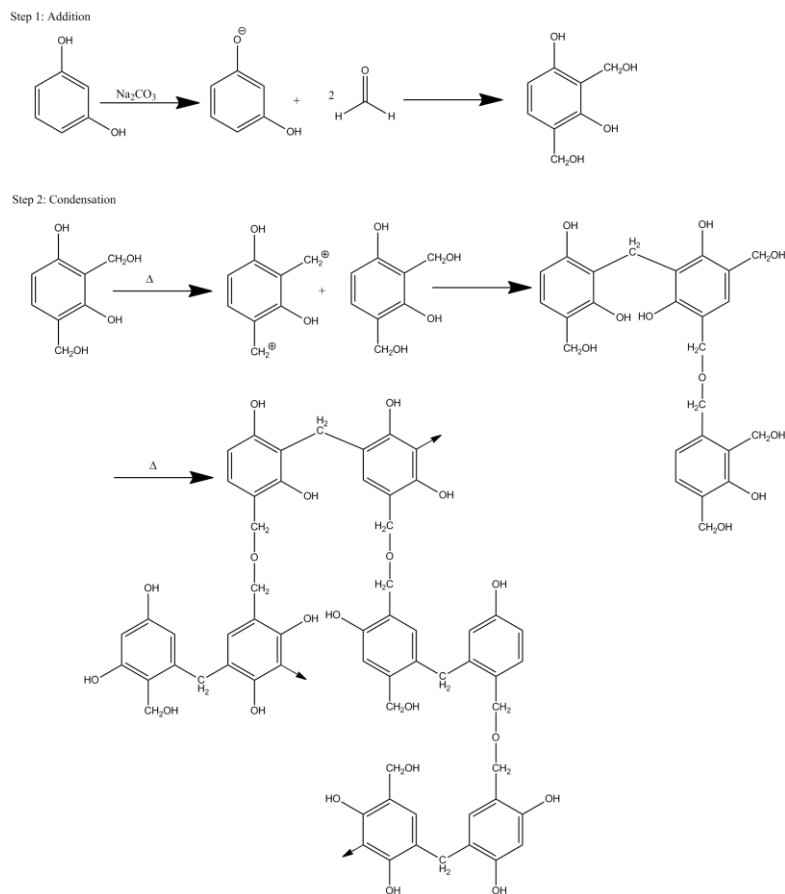


Figure 1. The general mechanism for RF gel network formation, as proposed by Al-Muhtaseb *et al.*¹⁴

An initial ortho-para addition step of 2 moles of formaldehyde to resorcinol in the presence of a mild base catalyst to notionally yield 2,4-bis(hydroxymethyl)benzene-1,3-diol. At elevated temperature, this species undergoes a series of poly-condensation reactions of the aromatic and aliphatic alcohol groups, eventually forming a high molar mass 3-D network (gel) of aromatic rings linked by methylene and ether bridges.

With new impetus towards the development of hierarchical graphene and CNT macro-assemblies for application in fields such as advanced energy storage and catalysis, there is much renewed interest in the organic sol-gel process. It is therefore both timely and necessary to examine these reactions in more detail and gain a more rigorous understanding of the mechanisms by which the initial organic network form, with the goal of obtaining improved control over the gelation structure. Indeed there is evidence that imperfections in the final inorganic carbon aerogel structures (e.g. the presence of residual organic

regions, microscopic nodes and micro-scale occlusions) are directly related to non-idealities in the organic precursor network.²³

In this study we have investigated the mechanism of the organic sol-gel network forming reaction of resorcinol and formaldehyde from a structural and kinetic standpoint by using a combination of real-time high field solution state nuclear magnetic resonance (NMR), low field NMR relaxometry and differential scanning calorimetry (DSC). These investigations have allowed us to track the network formation processes in real-time, gain both detailed structural information on the mechanisms of the RF sol-gel process and a quantitative assessment of the kinetics of the global network formation process.

2. EXPERIMENTAL

2.1 Materials. All reagents were used without further purification. Resorcinol (99%), formaldehyde (37% in water), DMSO-d₆ and TMS were purchased from Aldrich Chemical Co. Sodium carbonate (anhydrous) was purchased from J.T. Baker Chemical Co.

2.2 Preparation and sampling of resorcinol-formaldehyde gels. 11 wt. % resorcinol-formaldehyde (RF) gels were prepared in 20 mL glass vials and stored at temperatures ranging from 25-50°C. 200 μ L (or 200 mg if gelled) aliquots were collected along a series of time intervals from T_0 to T_∞ (24-96 H, dependent on the analysis temperature) during the gelation process and immediately quenched in 5 mL vials containing 1mL DMSO-d₆/(0.03%)TMS and dried in 0.5 g sodium sulfate. Gelled aliquots were swelled in DMSO-d₆/TMS by sonication prior to storage. Aliquots were stored in liquid nitrogen in order to quench any reactivity until such time as they were analyzed by NMR and DSC. 11 wt. % RF samples for T_2 relaxometry analysis were prepared in 5mm NMR tubes for in-situ analysis, with the addition of the catalyst to the solution defined as T_0 .

2.2 High field NMR measurements. Proton detected spectra were acquired immediately after being brought to 25°C from liquid nitrogen temperatures with a Bruker Avance III NMR spectrometer operating at 600 MHz and TopSpin 3.0 software, with samples sealed in high resolution 5.0 mm

Norell™ tubes rated for 600 MHz. All NMR spectra were collected with a Bruker Triple Resonance Broadband liquid capable gradient probe. NMR chemical shift reference: ^1H NMR, HD_2SOCD_3 : 2.50 ppm; $\text{C}_4\text{H}_{12}\text{Si}$: 0.00 ppm. All spectra were acquired at 298 K to impede further reaction progress during NMR acquisition. 1-D ^1H NMR spectra were collected with solvent suppression using the WATERGATE-W5 suppression sequence²⁴ with a total acquisition time (aq) of 183 s, a 2 s relaxation delay (d1) at 32 scans and 2 Hz exponential line broadening.

2.3 Low Field T₂ relaxometry. All T₂ relaxometry studies were performed on a low field Bruker Minispec™ spectrometer under static conditions using the Carr-Purcell-Meiboom-Gill (CPMG) spin echo method²⁵ with ninety degree pulse lengths of $\tau_P = 2.25\ \mu\text{s}$ and recycle delays of 15s. T₂ values were obtained from the mono-exponential fits of a train of collected FID's generated from the CPMG sequence. 2g Samples of 11 wt. % resorcinol-formaldehyde solution were prepared in 5mm borosilicate NMR tubes and allowed to equilibrate at the analysis temperature, in the probe for 2 minutes. T₂ measurements were then taken at variable time intervals (from 5 minutes to 12) hours over a total time period of 48 hours, at temperatures of 30, 35, 40, 45 and $50 \pm 0.1\ ^\circ\text{C}$ respectively. For each temperature, the values of T₂ were plotted as a function of time and fitted to an exponential decay curve to yield an effective rate of gelation of the system.

2.4 DSC analysis. All DSC characterization was carried out using a Perkin-Elmer Diamond DSC operating in non-modulated mode using power-compensation. Six milligram samples of 11 wt. % resorcinol-formaldehyde solution were prepared in sealed hermetic pans. The samples were prepared at 293K prior to analysis and were analysed using an isothermal temperature program with an initial 2 minute hold at 293K followed by a jump to 348K and a hold time of 20 minutes, under a N₂ purge flow.

3. RESULTS AND DISCUSSION

3.1 Solution state ^1H NMR characterization of organic precursors. In order to accurately study and assess the mechanism of the resorcinol-formaldehyde poly-condensation reaction, the purity and identity of the main reactants must first be determined. To that end, both the resorcinol and formaldehyde

starting materials have been characterized using high resolution ^1H -NMR: 17.61 ± 0.09 g/L and 25.4 ± 0.1 g/L. Solutions of resorcinol and the pre-prepared 37% aqueous formaldehyde solutions respectively, were prepared in d_6 -DMSO & D_2O for NMR analysis, both with and without the addition of 0.035 wt % sodium carbonate catalyst. NMR analysis of resorcinol in the absence of the catalyst, confirmed that the reagent was indeed $\sim 99\text{wt}\%$ benzene-1,3-diol, showed no evidence of dimerization or polymerization in aqueous solution and that both of the alcohol protons were in rapid exchange with an aqueous environment at 25°C . On the addition of the carbonate catalyst, a rapid colour change from clear to pale yellow was observable in all of the resorcinol solutions. No significant changes associated with this color change were detectable with NMR and it is attributed solely to the formation of the highly coloured $[\text{Na}^+]$ resorcinol salt on the addition of the sodium carbonate catalyst²⁶.

In contrast with resorcinol, the NMR analysis of the formaldehyde indicates that it is a complex mixture of species in a dynamic equilibrium with the aqueous environment. Shown in **Figures 2&3** are the ^1H -NMR spectra obtained for the aqueous formaldehyde precursor, with associated peak assignments given in **Table 1**.

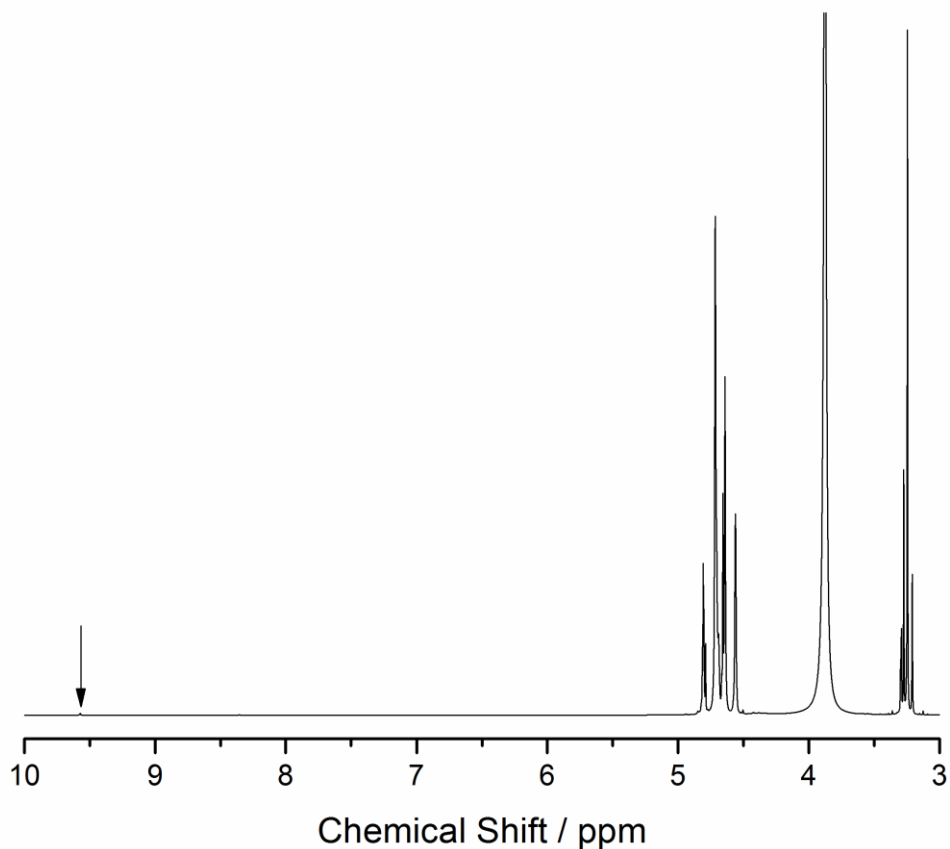


Figure 2. ^1H -NMR spectrum of the as prepared aqueous formaldehyde precursor in DMSO at 25°C, referenced to tetra-methyl silane (0 ppm). Note that the spectrum is complex and indicative of the presence of multiple chemical species. There are two main regions of proton intensity (which are expanded and discussed in **Figure 3**) and notably, the free formaldehyde proton signature (denoted by the arrow) is of extremely low relative abundance compared with the other species.

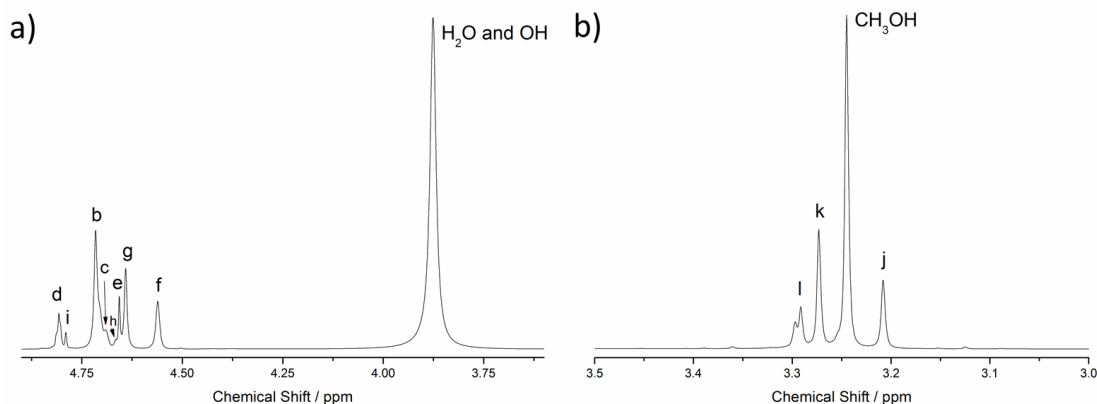


Figure 3. Expanded ^1H -NMR spectra of the as prepared aqueous formaldehyde precursor. Region a) is from 3.5 to 5 ppm and shows both the aliphatic alcohol protons of a series of oligo-ether diols and polyols. Region b) is expanded from 3-3.5 ppm and shows both a strong methanol signal and signals of protons associated with a second series of mono oligo-ether alcohols. Full peak assignments and relative abundances can be found in **Table 1**.

Table 1. Peak assignments, ^1H chemical shifts and relative abundances of the identified compounds in the 37% aqueous formaldehyde precursor material.

Compound	Chem. Shift (ppm)	% Abundance
CH_2O^*	A: 9.57	0.03
A		
$\text{HOCH}_2\text{OCH}_2\text{OH}$	B: 4.72	11.89
B B		
$\text{HOCH}_2\text{O}(\text{CH}_2\text{O})_n\text{CH}_2\text{OH}$	C: 4.71	1.61
C D	D: 4.81	2.82
HOCH_2OH	E: 4.66	2.17
E	F: 4.56	4.54
$\text{CH}_3\text{OCH}_2\text{OH}$	G: 4.64	5.58
J F	H: 4.69	0.54
$\text{CH}_3\text{OCH}_2\text{OCH}_2\text{OH}$	I: 4.79	0.68
K G H	J: 3.21	1.46
$\text{CH}_3\text{OCH}_2\text{OCH}_2(\text{OCH}_2)_n\text{OCH}_2\text{OH}$	K: 3.27	2.23
L G I D H	L: 3.29	0.79
CH_3OH	M: 3.24	6.18
M		

* Free formaldehyde

From these data shown in **Figures 2-3** and **Table 1**, two things are immediately apparent with respect to the composition and speciation of the formaldehyde precursor material: 1) In aqueous solution and at ambient temperatures, fully protonated formaldehyde is not the dominant molecular species. 2) What is typically thought of as ‘formaldehyde’ (CH_2O) in an aqueous environment is in fact a complex series of dimers-oligomers which range from methanol to oligomeric poly(oxymethylenes). The most abundant single species detected was methane diol, followed by methanol. Indeed, aqueous formaldehyde is often referred to as being in equilibrium with methane diol and having a significant methanol impurity present (with the latter often deliberately included as a polymerization inhibitor)²⁷. However, what the NMR analysis indicates is that the reality is even more complex; even in the presence of methanol, formaldehyde readily dimerizes and polymerizes to form a complex mixture of species. Despite this complexity, and given the reactivity of the reagent with respect to resorcinol, it is fair to assert that these conversion reactions in the formaldehyde reagent are to some extent reversible and low level of ‘free-formaldehyde’ exists, in aqueous solution, in a dynamic equilibrium with a series of complex and ill-defined polyether alcohols. The consequence however, for the resorcinol-formaldehyde network reaction is that we can no longer be certain of a quantitative reaction in terms available concentration of formaldehyde and we must also assume that the many diols and polyethers present are capable of participating in the condensation reactions. Therefore the very use of the formaldehyde reagent potentially adds significant complexity to the mechanism and uncertainty as to the nature of the final network structure.

3.2 In-situ chemical shift resolved NMR analysis of the RF network formation process. Through utilizing the sample and quench method described in the experimental section, an attempt was made to resolve the RF network formation process as a function of reaction time, using ^1H NMR. Given in **Figure 3** and **Tables 2** (respectively) are the time resolved ^1H spectra obtained from T_0 to T_∞ at 40°C and their accompanying peak assignments.

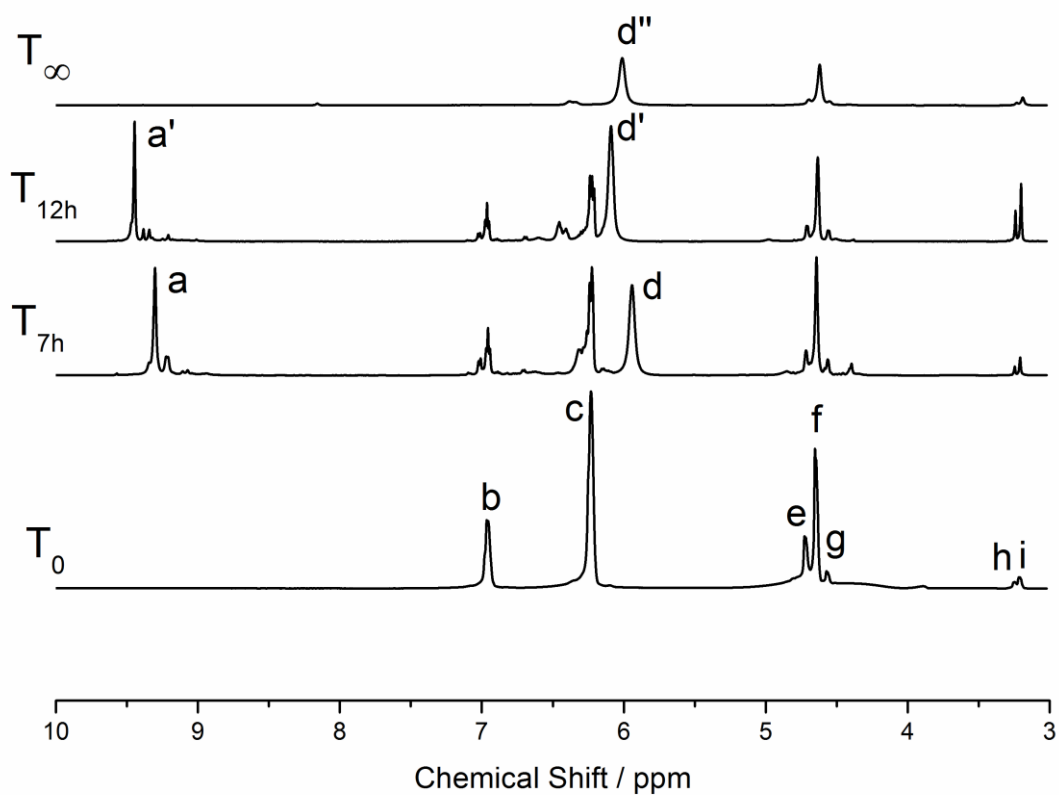


Figure 3. ^1H -NMR spectra of a series of time resolved samples of the 11Wt % RF system in DMSO with water suppression and referenced to tetra-methyl silane (0 ppm). Peaks labelled a-i represent major identified chemical species and are tabulated in **Table 2**.

Table 2. Peak assignments and ^1H chemical shifts of the identified species in the time resolved, sample aliquots of the 11% RF system studied at 40°C.

Species	Chemical Shift (ppm)
$\text{Ar-CH}_2\text{O}$	A: 9.30
	A': 9.45
	B: 6.95
Ar-H	C: 6.22
	D: 5.94
	D': 6.09
Ar-OH	D'': 6.01
	E: 4.72
	F: 4.64
$\text{Ar-CH}_2\text{OCH}_2\text{-Ar}$	G: 4.65
$\text{Ar-CH}_2\text{OH}$	I: 3.21
$\text{CH}_3\text{COCH}_2\text{OH}$	

From the ¹H data given in **Figure 3** and **Table 2** it is observed that even at T₀ significant levels of bond forming reactions have occurred (note the appearance of peaks E & F in **Figure 1**, attributed to aryl methoxy bridges and terminal aryl methyl-alcohol group formation). These data suggest that at 40°C there is an initial fast reaction between resorcinol and formaldehyde to produce both methyl alcohol substituted rings (as in **Figure 1**) and to begin the process of poly-condensation. After 7 hours at 40°C both a primary aromatic alcohol and an aromatic aldehyde species are observed to be present in the reaction samples. The clear presence of an aromatic aldehyde suggests that the reaction environment is somewhat more oxidizing than has previously been suggested and the methyl alcohol and related alcohol ring substituents may in fact be undergoing a significant degree of oxidation under the conditions of the gelation process. It has been observed that as these systems gel – we observe a darkening of the upper layers exposed to the atmosphere, with respect to the bulk of the gel sample. These observations support the case for some manner of oxidation occurring within the system during the timeframe of the network formation process. The presence of aldehydic species in the RF reaction matrix give rise to the possibility of secondary esterification reactions forming chemically distinct and potentially more labile network bridges and adds to the complexity of potential network architectures now possible.

Between 7 and 12 hours reaction time, significant downfield shifts in the aldehyde and alcohol peaks (a to a' and b to b') were also observed and are indicative of the increasing levels of substitution of the aromatic ring population as the polycondensation reaction proceeds. Finally, at T_∞ the increased substitution of the majority of the aromatic ring sites combined line broadening effects of the new heavily crosslinked matrix lead to an almost total loss of aromatic signal. The aldehyde protons are also no longer observable – suggesting either complete reaction or loss within the network and only those terminal, edge hydroxyl and alcohol protons that remain near the surface of the gel matrix are observable.

3.2 Time-temperature resolved NMR relaxometry analysis of the RF network formation process. The solution state NMR analysis of the gelation process broadly supports the accepted mechanism of addition of a formaldehyde type species to resorcinol in an initial fast step, followed by a series of poly-condensation reactions to form the gel matrix, however these analyses also indicated that the reaction does not proceed quantitatively due to the ill defined nature and reactivity of the formaldehyde starting materials and that there is the potential, in the presence of oxygen, for additional side reactions to occur. Through the use of T_2 relaxometry however, the global process of network formation has been followed over a range of temperatures, from an effective ' T_0 ' to T_∞ . Using a comparatively fast and simple static CPMG method, values of T_2 of the RF system as it gels have been obtained. The transverse relaxation time (T_2) can be thought of as proportional to the mobility of protons within the system of study, therefore the T_2 response is a convenient and sensitive probe of the relative mobility of the system and should respond to the changes on the motional dynamics of the RF system as it gels in real time. Shown in **Figure 4** is a plot of T_2 as a function of 'cure-time' for the RF system, studied at 50°C.

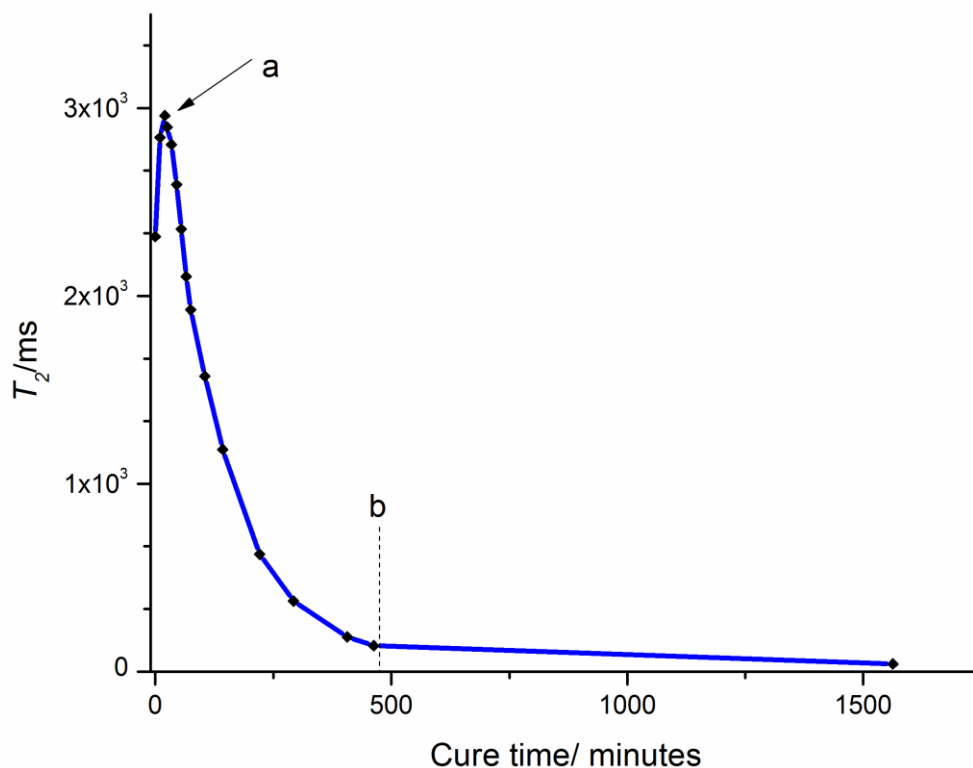


Figure 4. T_2 response as a function of experiment time at 50°C for the 11wt. % RF system, note that on addition of the catalyst there is a transient increase in the T_2 response (a), thought to be associated with a reaction exotherm. The T_2 response of the system then follows an exponential decay process as the network forms and molecular mobility correspondingly decreases. The gelation point is identified (b) and T_2 continues to decrease only very slowly after this point as the network densities.

From **Figure 4** it can be observed that there is a very obvious transient increase in T_2 at T_0 for the RF system. This transient increase is both repeatable and occurs over the range of temperatures studied (only if the catalyst is added). As T_2 is proportional to proton mobility, the most likely explanation therefore is that we are observing a reaction exotherm and this is in fact the case. Isothermal DSC confirms that on mixing of the catalyst with the RF precursors, there is in fact a detectable reaction exotherm. See **Figure 5**.

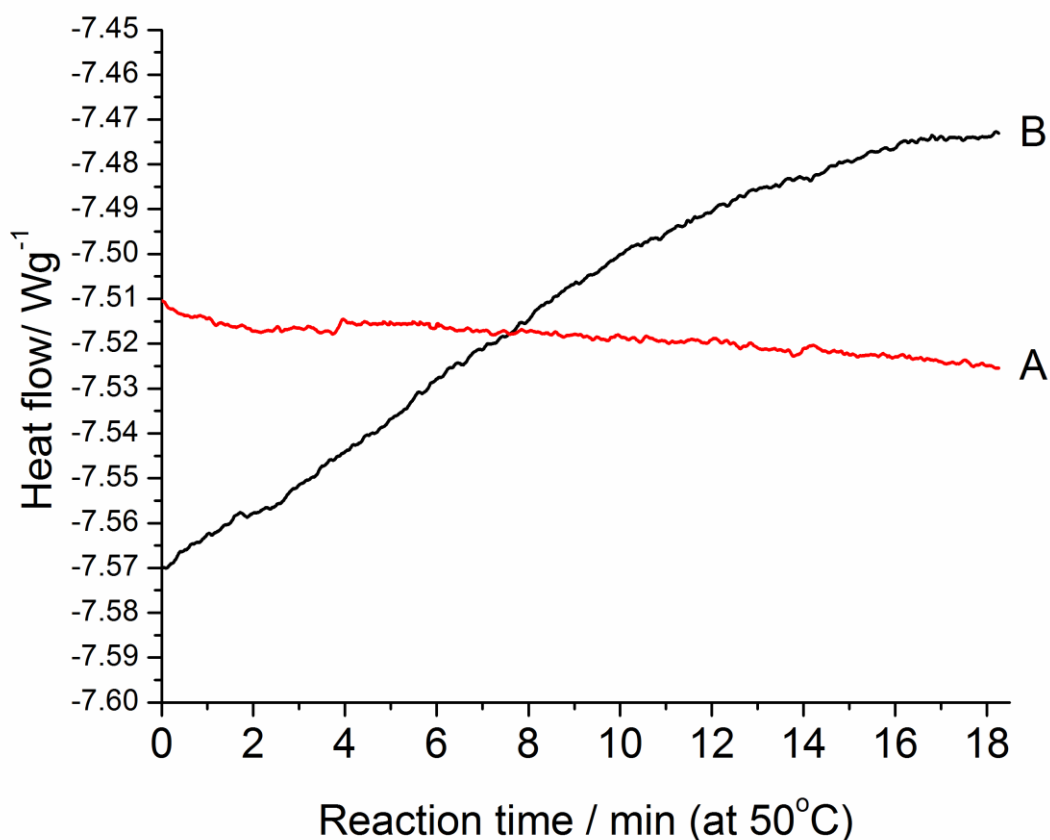


Figure 5. Isothermal DSC analysis of the 11Wt. % RF system at 50°C on the addition of the catalyst. (A) Is the isothermal profile of a 6mg water blank and (B) is the thermogram of a ~6mg sample of the 11Wt. % RF formulation, which was initially quenched then rapidly heated to 50°C. Note that there is a significant exotherm measured with respect to a water blank of the same mass.

The DSC analysis confirms that the initial increase in the T_2 values observed are a result of a fast exothermic step that occurs on the addition of the catalyst. These data are consistent with the solution state NMR analysis that suggested that new bond forming reactions (formation of aryl methoxy bridges and terminal aryl methyl-alcohol groups) occurred almost immediately on catalyst addition. From the DSC data, the measured peak enthalpy of 4.9 Jg^{-1} was used to calculate an estimated reaction enthalpy of this process of be $\sim 12.5 \text{ kJ mol}^{-1}$.

Returning to the relaxation data in **Figure 4**, it can be observed that the RF system follows a somewhat standard conversion curve for a thermoset network and the effective rate of network growth that the T_2 response is coupled to follows an exponential decay profile – typical of a poly-condensation network polymerisation process²⁸⁻³¹. The rate of the RF network formation process has a strong temperature dependence and to a large extent must be thermally driven at these concentrations to reach high degree of conversion. The strong temperature dependency of the poly-condensation reaction can be observed in **Figure 6** which graphs the T_2 decay curves for the RF systems, studied over a range of temperatures.

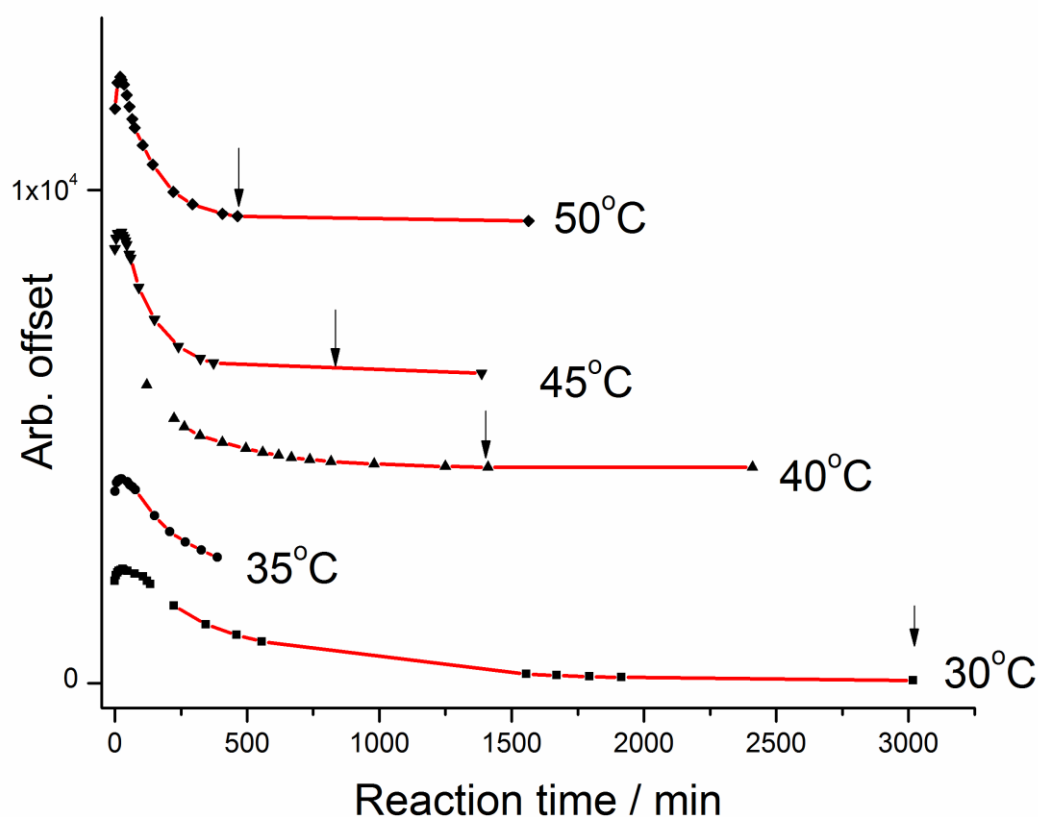


Figure 6. T_2 response as a function of reaction time and temperature for the 11wt. % RF system (30-50°C) Note that the initial exotherm is present in all systems; however the rates increase with increasing

temperature. Additionally, the effective time to gelation (indicated in each plot by an arrow) is observed to vary approximately as a quadratic function of temperature.

Over the range of temperatures studied, the RF polymerization reaction appears to obey classical network formation models^{31,32}. By fitting the T_2 data to a first order exponential function an effective rate for the network formation process may be obtained. This fitting has been executed for all of the data presented in **Figure 6** and the overall reaction has been shown to follow 1st order Arrhenius kinetics (see Figure 7).

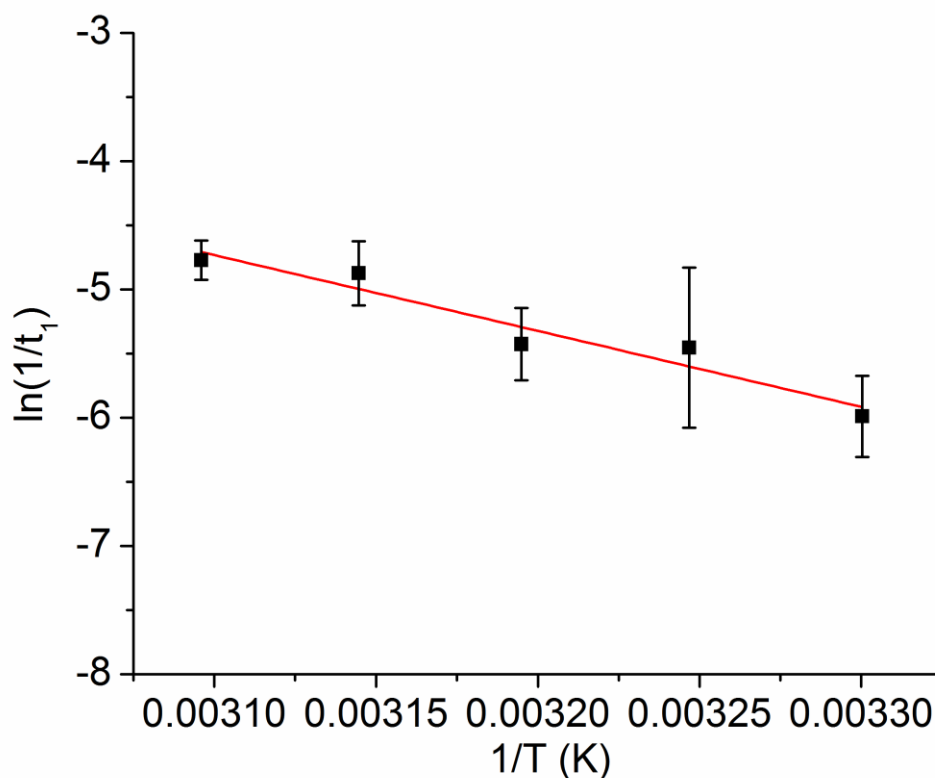


Figure 7. Natural log of the fitted exponential decay rates obtained from T_2 relaxometry data as a function of $1/T$ – where T is the reaction temperature. Observe that the reaction follows an Arrhenius kinetic model and a global ‘apparent’ activation energy for the network formation process was calculated to be $49 \pm 6 \text{ kJ mol}^{-1}$.

From kinetic treatment of the fitted relaxometry data, it is observed that the overall observed process of network formation in the 11 wt% RF systems has an apparent activation barrier of $49 \pm 6 \text{ kJ mol}^{-1}$. This process is the sum of the various condensation, coupling and other side reactions postulated and observed, which all contribute to the reduction in mobility of the system brought about by the progressive formation of a macromolecular network. Despite the initial exothermic addition step, the reaction must be thermally driven toward completion. However, over the temperature range in the study there does not appear to be a significant difference in the mechanistic process of network formation from a kinetic standpoint.

Overall, NMR-relaxometry and DSC analysis have shown that despite the complexity of the starting material and the complexity of the network formation reactions, the global process of network polymerization follows a classical, thermally driven poly-condensation model. This simple behaviour is due in great part to the large numbers of reactive groups (OH, active Ar-H and aldehyde) available for new bond formation and network growth, their effective high availability due to low molecular constraints, and the absence of cure-inhibitors or network termination species.

4. CONCLUSIONS

The base-catalysed reaction between dilute aqueous resorcinol and formaldehyde to form an organic sol-gel, despite generally being considered to be a simple poly-condensation network formation reaction, is in fact a complex and inherently ill-defined process. This complexity is a result of both the molecular diversity of aqueous solutions of formaldehyde and the wide range of reactions and side reactions that can occur during network polymerization. We have shown that the RF-gelation process proceeds through a rapid exothermic initial step to form significant quantities of aryl methoxy bridges and terminal aryl methyl-alcohol groups. Further reactions result in increased substitution of the aryl ring systems, further formation of bridging methoxy structures and the overall formation of a crosslinked 3D network. It is very likely that this poly-condensation process is further complicated through the participation of a wide range of diol/polyol ‘impurities’ from the formaldehyde precursor.

There is also evidence from the presence of aldehydic species, that oxygen plays an active role in the network formation process and organic RF gel systems in-fact contain a significant percentage of oxidised functionality. Despite the structural complexity of the RF gelation process, the results of NMR relaxometry studies have shown that the global network formation reaction, from a kinetic standpoint, closely approximates that of a classical poly-condensation reaction.

Despite the robust nature of the RF sol-gel reaction, the results of these investigations suggest strongly that further control of the final network structure may be impossible when using formaldehyde and a poly-condensation process. Exclusion of oxygen may alleviate the aldehyde formation side-reaction - resulting in some improvements in network structural order, however the fact that formaldehyde exists in aqueous solution, in a complex equilibrium with a range of other reactive compounds, fundamentally limits the molecular control one can obtain over the precise nature of the final RF gel structure. Alternative precursor molecules to formaldehyde (long-chain aldehydes or diacids) or the use of irreversible ‘click’ chemistries such as vinyl addition may ultimately yield tighter control over the organic network structure, however these alternatives may be significantly more synthetically complex and ultimately less robust than the RF process.

5. ACKNOWLEDGEMENTS

This work was performed under the auspices of the U.S. Department of Energy by Lawrence Livermore National Laboratory under Contract DE-AC52-07NA27344. The authors would also like to gratefully acknowledge Mark Pearson (LLNL) for his assistance in carrying out the TGA of the materials studied.

The authors would like to thank Matthew Kaiser (US Army, West Point Academy) for his assistance with sample quenching.

6. REFERENCES

- (1) Wen, J.; Wilkes, G. L. *Chemistry of Materials* **1996**, 8, 1667.
- (2) Pekala, R. W.; Alviso, C. T.; Kong, F. M.; Hulsey, S. S. *J. Non-Cryst. Solids* **1992**, 145, 90.

- (3) Frackowiak, E.; Beguin, F. *Carbon* **2001**, 39, 937.
- (4) Lazzari, M.; Soavi, F.; Mastragostino, M. *J Power Sources* **2008**, 178, 490.
- (5) Pekala, R. W.; Farmer, J. C.; Alviso, C. T.; Tran, T. D.; Mayer, S. T.; Miller, J. M.; Dunn, B. *Journal of Non-Crystalline Solids* **1998**, 225, 74.
- (6) Koebel, M.; Rigacci, A.; Achard, P. *J Sol-Gel Sci Technol* **2012**, 63, 315.
- (7) Biener, J.; Stadermann, M.; Suss, M.; Worsley, M. A.; Biener, M. M.; Rose, K. A.; Baumann, T. F. *Energy Environ. Sci.* **2011**, 4, 656.
- (8) Lambert, S.; Job, N.; D'Souza, L.; Pereira, M. F. R.; Pirard, R.; Heinrichs, B.; Figueiredo, J. L.; Pirard, J. P.; Regalbuto, J. R. *J Catal* **2009**, 261, 23.
- (9) Meena, A. K.; Mishra, G. K.; Rai, P. K.; Rajagopal, C.; Nagar, P. N. *Journal of Hazardous Materials* **2005**, 122, 161.
- (10) Kucheyev, S. O.; Google Patents: 2013.
- (11) Pauzuskie, P. J.; Crowhurst, J. C.; Worsley, M. A.; Laurence, T. A.; Kilcoyne, A. L. D.; Wang, Y. M.; Willey, T. M.; Visbeck, K. S.; Fakra, S. C.; Evans, W. J.; Zaug, J. M.; Satcher, J. H. *P Natl Acad Sci USA* **2011**, 108, 8550.
- (12) Worsley, M. A.; Kucheyev, S. O.; Satcher, J. J. H.; Hamza, A. V.; Baumann, T. F. *Applied Physics Letters* **2009**, 94, 073115.
- (13) Worsley, M. A.; Pauzuskie, P. J.; Olson, T. Y.; Biener, J.; Satcher, J. H.; Baumann, T. F. *Journal of the American Chemical Society* **2010**, 132, 14067.
- (14) Al-Muhtaseb, S. A.; Ritter, J. A. *Advanced Materials* **2003**, 15, 101.
- (15) Kelts, L. W.; Armstrong, N. J. *Journal of Materials Research* **1989**, 4, 423.
- (16) Corriu, R. J. P.; Leclercq, D. *Angewandte Chemie International Edition in English* **1996**, 35, 1420.
- (17) Kelts, L. W.; Effinger, N. J.; Melpolder, S. M. *Journal of Non-Crystalline Solids* **1986**, 83, 353.
- (18) Livage, J.; Sanchez, C. *Journal of Non-Crystalline Solids* **1992**, 145, 11.
- (19) ElKhatat, A. M.; Al-Muhtaseb, S. A. *Advanced Materials* **2011**, 23, 2887.
- (20) Werstler, D. D. *Polymer* **1986**, 27, 757.
- (21) Šebenik, A.; Osredkar, U.; Vizovišek, I. *Polymer* **1981**, 22, 804.
- (22) Raff, R. A. V.; Silverman, B. H. *Industrial & Engineering Chemistry* **1951**, 43, 1423.
- (23) Kim, S. J.; Hwang, S. W.; Hyun, S. H. *Journal of Materials Science* **2005**, 40, 725.
- (24) Liu, M.; Mao, X.-a.; Ye, C.; Huang, H.; Nicholson, J. K.; Lindon, J. C. *Journal of Magnetic Resonance* **1998**, 132, 125.
- (25) Maus, A.; Hertlein, C.; Saalwachter, K. *Macromolecular Chemistry and Physics* **2006**, 207, 1150.
- (26) Krauskopf, F. C.; Ritter, G. *Journal of the American Chemical Society* **1916**, 38, 2182.
- (27) Dankelman, W.; Daemen, J. M. H. *Analytical Chemistry* **1976**, 48, 401.
- (28) Yousefi, A.; Lafleur, P. G.; Gauvin, R. *Polymer Composites* **1997**, 18, 157.
- (29) Nzihou, A.; Sharrock, P.; Ricard, A. *Chemical Engineering Journal* **1999**, 72, 53.
- (30) Chern, C. S.; Poehlein, G. W. *Polymer Engineering & Science* **1987**, 27, 788.
- (31) Flory, P. J. *Principles of Polymer Chemistry*
Cornell University, 1953.
- (32) Mikes, J.; Dusek, K. *Macromolecules* **1982**, 15, 93.